Minimal conformation of the α-conotoxin ImI for the α7 neuronal nicotinic acetylcholine receptor recognition: correlated CD, NMR and binding studies

Hung Lamthanh[a,*], Christelle Jegou-Matheron[b], Denis Servent[a], André Ménez[a], Jean-Marc Lancelin[b]

[a] *CEA, Département d'Ingénierie et d'Etudes des Protéines, CE Saclay, Bâtiment 152, 91191 Gif sur Yvette Cedex, France*
[b] *Laboratoire de RMN Biomoléculaire associé au CNRS, Université Claude Bernard-Lyon 1 and Ecole Supérieure de Chimie, Physique et Electronique de Lyon, Bâtiment 308G, 69622 Villeurbanne Cedex, France*

Received 24 April 1999; received in revised form 3 June 1999

Abstract **The α-ImI conotoxin, a selective potent inhibitor of the mammalian neuronal α7 nicotinic acetylcholine receptor (n-AchR), was shown by point mutation or by L-alanine scanning to display two regions essential for bioactivity: the active site Asp[5]-Pro[6]-Arg[7] in the first loop and Trp[10] in the second loop. The deletion of the Cys[3],Cys[12] disulfide bond in the α-ImI scaffold, e.g. peptide II, had no effect on its binding affinity. CD spectra, NMR studies and structure calculations were carried out on the wild type α-ImI, the weakest analog (R7A) and peptide II (equipotent to α-ImI) in order to point out the conformational differences between these compounds. Then, an attempt to correlate the conformational data and the affinity results was proposed. CD and NMR data were identical for the R7A analog and α-ImI, revealing the crucial functional role of the Arg[7] side chain. On the other hand, the scaffold of the first loop in peptide II was shown by NMR to represent the minimal conformation for the optimal interaction of the toxin with the neuronal α7 n-AchR. Last, the β-turn forming property of the 6th residue (Pro) in the active site of the α-ImI can be correlated with its affinity.**

Key words: α-Conotoxin; α7-Nicotinic acetylcholine receptor; Binding affinity; Circular dichroism; Nuclear magnetic resonance

1. Introduction

α-Conotoxins, isolated from venomous marine cone snails, are small disulfide-rich peptides which block, like the α-neurotoxins from snake venoms, the nicotinic acetylcholine receptor (n-AChR) at the neuromuscular junction and lead to flaccid paralysis. The best characterized examples of α-conotoxins are α-GI and α-MI conotoxins (for a review see [1]). Recently, new α-conotoxins which do not interact with the muscular receptor but specifically with different neuronal n-AChR subtypes were discovered. The α-ImI from *Conus imperialis* [2], α-EpI from *Conus episcopatus* [3], α-MII from *Conus magus* [4], and α-AuIB from *Conus aulicus* [5] are selective potent inhibitors of mammalian neuronal n-AChR of the α7, the α3β2, the α3β4, the α3β2 and the α3β4 subtypes, respectively (Fig. 1). On the other hand, two α-conotoxins from *Conus pennaceus* (α-PnIA and α-PnIB) block specifically the neuronal AChR in mollusc [6].

α-ImI was reported to have negligible effects on the mammalian neuromuscular transmission whereas after i.c.v. injection in rat it causes complex seizures by high affinity blocking of the neuronal homomeric α7 n-AchR [2,7,8]. Recently, α-ImI mutants either by L-alanine scan [9] or point mutations [10] were synthesized and their binding affinity was measured. The results revealed two key regions in α-ImI essential for bioactivity: the sequence $D^5P^6R^7$ is a major determinant assisted by the W^{10} residue [9,10]. Furthermore, the deletion of the disulfide bond (Cys^3,Cys^{12}) had no effect on the toxin affinity as reported for peptide II [9] in which Cys^2,Cys^8 were bridged and Cys^3,Cys^{12} were acetamidomethylated (Fig. 1). On the other hand, the additional deletion of the (Cys^2,Cys^8) disulfide bond caused a 17-fold affinity decrease for peptide I [9] in which Cys^2,Cys^8 were carboxamidomethylated and Cys^3,Cys^{12} were acetamidomethylated (Fig. 1). Therefore, the first loop $C^2CSDPRC^8$ is important for the binding affinity. This first loop was located in a distorted helix $D^5PRCAWR^{11}$ according to the 3D structure of the α-ImI [11,12].

From previous binding results of α-ImI [9,10] and the 3D structure of α-ImI [11,12], a question arises about the conformation of α-ImI after successive mutations of the active site residues in the first loop (D^5,P^6,R^7). The other question concerns the structural role of the Cys^2,Cys^8 disulfide bond in the binding affinity of the α-ImI. To address these questions, we carried out CD measurements of the L-Ala series of α-ImI analogs, various mutants in the active site (D5N, P6S, R7K), peptide I and peptide II. Simultaneously, a comparative NMR study of α-ImI, monodisulfide (Cys^2,Cys^8) peptide II, and the R7A analog was conducted. Together, the comparative CD and NMR methods enabled a possible correlation between the conformation of α-ImI and its binding affinity and allowed the understanding of the structural role of each residue in the active site of α-ImI and its selectivity for the α7 n-AchR.

2. Materials and methods

2.1. Solid phase peptide synthesis

Conotoxin α-ImI and analogs were synthesized by solid phase using

*Corresponding author. Fax: (33) 1 69 08 91 37.
E-mail: lamthanh@dsvidf.cea.fr

Abbreviations: Fmoc, fluorenylmethyloxycarbonyl; n-AchR, nicotinic acetylcholine receptor; S-cam, *S*-carboxymethyl; S-acm, *S*-acetamidomethyl; Nle, L-norleucine; CD, circular dichroism; HEK, human embryonic kidney; i.c.v., intracerebroventricular injection; DQF-COSY, double quantum filtered correlation spectroscopy; NOESY, nuclear Overhauser enhancement spectroscopy; rmsd, root mean square deviation; TOCSY, total correlation spectroscopy

0014-5793/99/$20.00
PII: S0014-5793(99)00831-5

α-Conotoxins	Sequence	loop sizes	Species	Receptor target	Ref.
				neuronal	
α-ImI	GCCSDPRCAWR----C-NH_2	4/3	*C.imperialis*	α7	[2]
α-EpI	GCCSDPRCNMNNPDYC-NH_2	4/7	*C.episcopatus*	α3/β2;α3/β4	[3]
α-MII	GCCSNPVCHLEHSNLC-NH_2	4/7	*C.magus*	α3/β2	[4]
α-PnIA	GCCSLPPCAANNPDYC-NH_2	4/7	*C.pennaceus*	*mollusc*	[6]
α-PnIB	GCCSLPPCALSNPDYC-NH_2	4/7	*C.pennaceus*	*mollusc*	[6]
α-AuIB	GCCSYPPCFATNPD-C-NH_2	4/7	*C.aulicus*	α3/β4	[5]
				muscular	
α-GI	ECCN-PACGRH--YSC-NH_2	3/5	*C.geographus*	α/δ, α/γ	[1]
α-GIA	ECCN-PACGRH--YSCGK-NH_2	3/5	*C.geographus*	α/δ, α/γ	[1]
α-MI	GRCCH-PACGKN--YSC-NH_2	3/5	*C.magus*	α/δ,α/γ	[1]
α-SI	ICCN-PACGPK--YSC-NH_2	3/5	*C.striatus*	α/δ,α/γ	[1]
α-SIA	YCCH-PACGKNF--DC-NH_2	3/5	*C.striatus*	α/δ,α/γ	[1]
α-SII	GCCCN-PACGPN--YGCGTSCS	3/5	*C.striatus*	α/δ,α/γ	[1]

Peptide I

GC(Scam)C(Sacm)SPDRC(Scam)AWRC(Sacm)-NH_2

Peptide II

GCC(Sacm)SDPRCAWRC(Sacm)-NH_2

Abbreviations:Scam,S-carboxamidomethyl;S-acm,S-acetamidomethyl; O = hydroxyproline.

Fig. 1. α-Conotoxin sequences, loop sizes, species of origin and n-AchR targets.

the Fmoc chemistry. The details of synthesis and purification have already been reported [13]. The linear peptide $Cys^{2,8}$(S-cam) $Cys^{3,12}$(S-acm) or peptide I were prepared by reaction of an excess of iodoacetamide with the $Cys^{2,8}$,$Cys^{3,12}$(S-acm) peptide in 0.1 M Tris-HCl buffer pH 8 and purified by HPLC. The overall yield of the α-ImI conotoxin and analogs ranged from 10 to 11% calculated from the starting Fmoc-Rink-AM-amide resin obtained from Novabiochem (Switzerland). Synthetic α-ImI and analogs were characterized by amino acid analysis, analytical HPLC and electrospray ionization mass spectrometry.

2.2. α7 Neuronal homooligomer AChR expression in HEK cells

The chimeric neuronal α7-5HT3 receptor is expressed transiently in HEK cells as described previously [14]. The cDNA of the α7-5HT3 receptor was kindly provided by Prof. J.P. Changeux (Institut Pasteur, Paris).

2.3. Binding assays

The inhibition of ^{125}I-bungarotoxin (^{125}I-Bgtx) binding to the α7 AChR by α-ImI conotoxin was measured by competition experiments as described previously [14].

2.4. Circular dichroism measurements

CD spectra were recorded on a Jobin Yvon CD6 dichrograph by accumulating 20 scans obtained with an integration time of 0.5 s every 0.2 nm. Peptide concentration was in the range of 0.5–1.0 mg/ml of sodium phosphate buffer (50 mM) at pH 7. Due the low solubility of the Nle^7 analog in aqueous solvent, its CD spectrum was recorded in a mixture of acetonitrile and phosphate buffer (50/50). The pathlength of the quartz cell is 0.2 mm and the ellipticity is expressed in deg cm^2 $dmol^{-1}$.

2.5. NMR spectroscopy

Peptides were dissolved at 5–6 mM concentrations in 90% H_2O/10% D_2O, 0.1 M potassium phosphate buffer pH 5.8. The NMR spectra were recorded at 5°C on a Bruker Avance DRX 500 spectrometer with a 5 mm (^{1}H, ^{13}C, ^{15}N) triple resonance probe head, equipped with a self shielded *z*-gradient coil. DQF-COSY [15], TOCSY [16,17] and NOESY [18,19] experiments were recorded with 512 (t_1)×1024 (t_2) complex data points. The spectral width was 11.0 ppm in both dimensions. Data were processed using the GIFA V.4 software [20]. Chemical shifts were referenced relative to H_2O at 5°C (4.964 ppm). The mixing time was 80 ms for the clean-TOCSY experiments [21] and 150 or 300 ms for NOESY experiments. Water suppression in TOCSY and NOESY experiments was performed by the WATERGATE sequence using a 3-9-19 pulse sequence with *z*-gradients [22,23], while a low-power presaturation was used during the relaxation delay of the DQF-COSY experiments. The quadrature detection in the t_1 dimension was achieved using the States-TPPI method [24]. Interproton distance constraints were derived from the cross-peak intensities of the NOESY spectrum recorded with a mixing time of 150 ms, and were classified into four categories, strong, medium, weak and very weak, as previously described [25]. The intensities of the NOESY cross-peaks corresponding to the distances H5-6, H4-5 and H6-7 of tryptophan were used as references for the strong category.

2.6. Structure calculations

The proposed models of the three peptides α-ImI, R7A analog and

peptide II were calculated using the program X-PLOR version 3.851 [26] and were analyzed using the MOLMOL 2.4 program [27] as previously described [25]. The structures were generated using consecutively the force fields *parallhdg.pro* and CHARMM22 of X-PLOR. A total of 84 (53 sequential (i, i+1), 20 medium-range (i, i+n, $n<5$), six long-range (i, i+n, $n>4$) and five intra-residue), 68 (46 sequential, 15 medium-range, four long-range, and three intra-residue) and 81 (46 sequential, 24 medium-range, seven long-range, and five intra-residue) structurally relevant distance restraints were used for the structure calculations of α-ImI, R7A analog and peptide II, respectively. Dihedral angle restraints were also used to restrain five χ_1 angles for the residues C^3, D^5, R^7, C^8 and W^{10} of α-conotoxin ImI. Three χ_1 angles restrained residues C^3, D^5 and W^{10} of the R7A analog and four χ_1 angles restrained residues C^3, D^5, R^7 and R^{11} of peptide II. No inter-residue NOEs were found for protons of thioacetamidomethyl groups of residues C^3 and C^{12} of peptide II. These groups were modelled as thiomethyl groups. Modelling of peptide II in which the thioacetamidomethyl groups of residues C^3 and C^{12} were modelled as two SH groups led to structures with the same scaffold as those described in this report (data not shown).

3. Results and discussion

As previously demonstrated by chemical site-directed mutagenesis experiments, three central residues D5, P6, R7 are crucial in the interaction of α-ImI with the α7 n-AchR [9,10]. Thus, the mutations of these residues cause at least a two orders of magnitude decrease in affinity. The W10 residue contributed more moderately to the binding activity as shown by the three- and six-fold affinity decrease observed respectively for the W10F and W10A analogs [9,10]. Conversely, the W10T analog have a 30-fold reduced affinity [10]. These observations emphasized the necessary presence of an aromatic or hydrophobic side chain at the 10th position in the second loop of α-ImI.

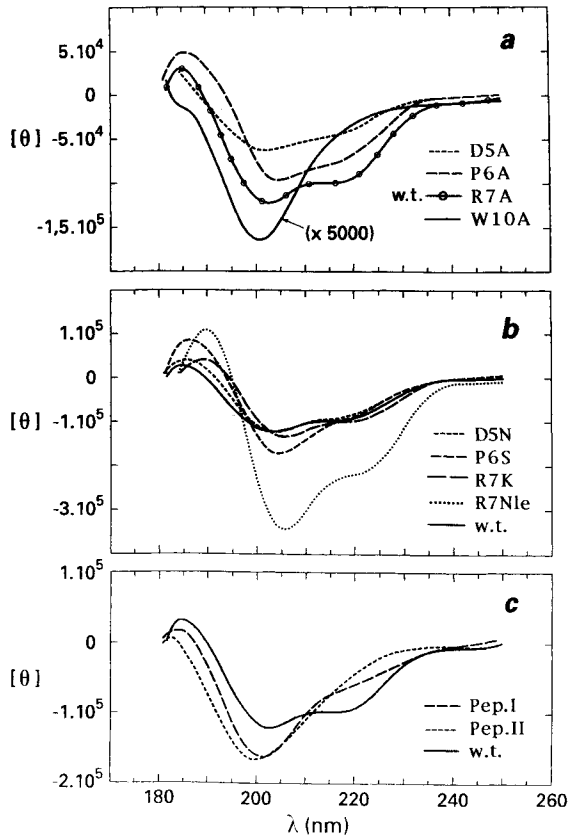

Fig. 2. CD spectra in the far UV region (180–250 nm) of the α-ImI conotoxin and analogs in aqueous buffer solution (50 mM sodium phosphate, pH 7). a: CD spectra of four L-Ala analogs: D5A, P6A, R7A, W10A α-ImI analogs and the w.t. α-ImI. The CD signals of the W10A analog were amplified 5000 times for comparison. b: CD spectra of four L-Xxx analogs: D5N, P6S, R7K analogs and the w.t. α-ImI. The R7Nle analog spectra was recorded in acetonitrile/buffer (1/1). c: CD spectra of peptide II and peptide I and the w.t. α-ImI.

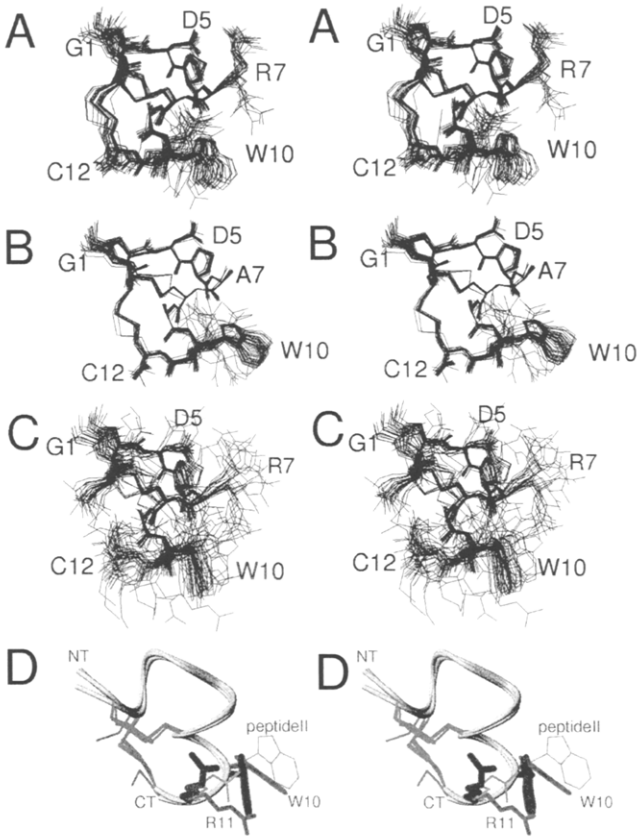

Fig. 3. Stereoviews of the NMR structures of α-ImI conotoxin and its derivatives (all heavy atoms) superimposed from residue Cys^2 to Cys^{12}, for minimum (N, Cα, C) atomic rmsds. A: wild type (30 models); B, R7A analog (27 models); C, peptide II (32 models). In D, the three closest structures to the geometric average of A, B, and C are superimposed each together using a MOLMOL ribbon presentation. The side chain heavy atoms of cysteines, Arg^{11} and Trp^{10} are presented as thick lines, medium lines, and thin lines for the wild type α-ImI, the R7A analog and the peptide II with Cys^3 and Cys^{12} alkylated, respectively (see text). Nt and Ct represent the N-termini and C-termini.

In order to attribute the affinity decrease observed for the mutation in the active site ($D^5P^6R^7$) and the W^{10} residue of α-ImI [9,10] to a modification of the recognition process rather than a general structural perturbation, CD of different analogs of the active site was carried out in comparison to that of the native α-ImI. The CD spectrum of α-ImI at neutral pH displayed two negative bands π-π* between 200 and 210 nm and n-π* near 220 nm (Fig. 2a). The spectrum resembles that of the α-helix [28] except that the band intensities and ratio are different. This CD feature is a class C (helix-like) CD spectrum [29] and indicates the presence of type I β-turn as has been shown by study of model peptides [30]. The NMR-established structure of α-ImI consists of the C^2CSD^5 type I β-turn followed by a distorted helix $D^5PRCAWR^{11}$ which is

Table 1
Structural statistics for the structures[a] of α-conotoxins ImI, ImIR7A and pepII in H_2O, pH 5.8 at 5°C

	α-ImI	α-ImIR7A	α-pepII
Cartesian coordinate rmsd (Å) vs. the average coordinates of the (N, C^{α}, C) backbone atoms of the calculated structures[a]			
Residues 1–12	0.78 ± 0.28	0.48 ± 0.17	1.49 ± 0.94
Residues 2–8	0.30 ± 0.13	0.18 ± 0.06	0.49 ± 0.33
X-PLOR potential energies (kcal mol^{-1}) (average ± S.D.) calculated with the *allhdg.pro* force field			
F_{TOTAL}	−122.57 ± 3.80	−119.88 ± 3.00	−125 ± 6.22
F_{BOND}	4.54 ± 0.35	4.47 ± 0.25	4.17 ± 0.26
F_{ANGLE}	21.62 ± 1.94	20.43 ± 1.38	20.33 ± 2.11
F_{IMPR}	0.84 ± 0.19	0.78 ± 0.09	0.86 ± 0.27
$F_{COULOMBIC}$	−180.29 ± 5.15	−183.29 ± 4.49	−182.53 ± 4.35
F_{NOE}	0.17 ± 0.10	0.31 ± 0.07	0.48 ± 0.20

*F*TOTAL: total energy; F_{BOND}: bond length deviation energy; F_{ANGLE}: valence angle deviation energy; F_{IMPR}: deviation energy for the improper angles used to maintain the planarity of certain groups of atoms; *F*COULOMBIC: Coulombic energy contribution; F_{NOE}: experimental NOE function calculated using a force constant of 50 kcal mol^{-1} $Å^{-2}$; F_{CDIH}: experimental function corresponding to the violation of the dihedral angle constraints.
[a]Respectively 30, 27 and 32 structures for α-conotoxins ImI, ImIR7A and pepII.

composed by a half turn S^4DPR^7 and R^7CAW^{10} type I β-turn [11,12]. The whole sequence is folded by two disulfide bonds Cys^2,Cys^8 and Cys^3,Cys^{12}. Therefore, the overall conformation in solution of α-ImI deduced from CD data can be assigned as a highly constrained and distorted helix [11,12].

The observed CD patterns for several analogs of α-ImI, modified in the active site D^5PR^7 did not reveal a great disorder of the helix-like spectra for D5N, P6S, the R7K analogs, except for the increased Cotton effect of the R7Nle analog due probably to the solvent effect, i.e. acetonitrile (Fig. 2b). In spite of the helix-like CD spectra of the P6S and P6A analogs (Fig. 2a,b), the structural role of Pro^6 in the loss of activity of these two analogs is obvious due to the substitution of the corner residue Pro^6 that contributed to decrease the high β-turn propensity of the D^5PRC^8 tetrapeptide [31]. In fact, the proline residue and two disulfide bonds force the α-ImI backbone to form continuous turns in helicoidal motifs [11,12]. Therefore, the loss of affinity going from P6S to P6A analogs can be correlated with the structural aspect. The lower the potential of turn forming at the 6th position of α-ImI, the higher is the loss of affinity. Two striking CD features were observed for L-Ala analogs of α-ImI. The CD spectrum of the R7A analog was superimposable on that of the α-ImI (CD measurements were carried out with the same accuracy in two separate experiments) (Fig. 2a). Therefore, the difference in binding affinity between the wild type and the R7A analog was only due to the side chain difference rather than structural modification. The conformation of these two molecules could be considered identical, and this was further confirmed by the NMR study. The second different CD pattern is displayed by the W10A analog. The two bands of the helix-like CD spectrum disappeared while one negative band around 200–205 nm appeared and has three orders of magnitude smaller than that of α-ImI. This observation can be related to (i) the deletion of the strong contribution of the aromatic Trp^{10} residue to the Cotton effect at 220 nm [32], (ii) the probable loss of the capacity of H-bond forming for NH(Ala^{10})/NH(Trp^{10}) with the CO(Pro^6) [11,12]. Therefore, the CD spectrum of the W10A analog can be considered a CD pattern of a β-turn structure similar to that of the model cyclo (d-Ava-Gly-Pro-Ser(OBu^t)-Gly) peptide [33].

Peptide I and peptide II displayed CD spectra (λ_{min} at around 200–205 nm) with a profile resembling that of the W10A analog (Fig. 2c). It might be hypothesized that peptides I and II contain a certain fraction of β-turn imposed by the sequence D^5PRC^8 [31]. Peptide I is probably more flexible and is less active than peptide II. Peptide II could preserve, more easily than peptide I, the two (4 → 1) H-bonds characteristic of a β-turn, NH(Asp^5)-CO(Cys^2), NH(Cys^8)-CO(Asp^5) detected in the 3D structure [11,12]. Thus, the first loop of peptide II can form the same helix-like conformation as in the native α-ImI. The cluster of the side chains of the active site $D^5P^6R^7$ can point in the same direction as in the native α-ImI. This comparison enabled the understanding of the conformational role of the first loop in α-ImI for its affinity. This was further verified by NMR.

The sequence-specific resonance assignments of the α-ImI, the R7A analog and peptide II were easily obtained [34]. The resonance of the Cys^2 amide proton of α-ImI and R7A analog is not observed probably due to an extensive chemical exchange with the solvent. The respective Cys^2 amide proton resonances of these two molecules are, however, observed on the fingerprint regions of their NOESY spectra recorded at 5°C. The two Hα to Hβ connectivities of Cys^2 are well identified in the aliphatic regions of both TOCSY and NOESY spectra (data not shown). Efficient magnetization transfers are observed for all nine other observable spin systems. The TOCSY spectra of the R7A analog is very similar to that of α-ImI showing that the chemical shift difference is minimal. Protons of the side chain of Arg^{11} are shifted to high field suggesting a contribution of the ring current anisotropy of Trp^{10}. Hα chemical shifts of peptide II differ more importantly particularly in C-terminal residues like Arg^{11} and Cys^{12}. This could result from the opening of the second disulfide bridge and the thiol alkylation. The peptide II presents a greater chemical shift dispersion in the NH-(*F*2) dimension mainly for residues 3–5, 8–9 and 11–12. Finally, the presence of strong Hα-to-Hδ,δ′(*i*+1) NOE between D^5 and P^6 with no Hα-Hα(*i*+1) cross-peak in the NOESY spectra indicates a unique *trans* conformation for the D^5-P^6 peptide bond of α-ImI, R7A analog and peptide II, in agreement with the results recently reported for the wild type α-ImI [11,12].

Fig. 3 shows the structures calculated for the three studied compounds that conform to both the experimental and the force-field restraints, and have no individual and systematic NOE violation exceeding 0.1 Å. The values of total potential energies of each structure lie around −120 kcal mol^{-1} as indicated in Table 1. The (ϕ, ψ) dihedral angles of the 3D

structures of α-ImI resulting from our work superpose exactly with the two other NMR structures described recently [11,12]. However, the three models differ slightly by the well-defined χ_1 values of residues Asp^5 (-178 ± 3) and Trp^{10} (61 ± 5) compared to the highly mobile side chain described by Maslennikov et al. [11]. Other differences for Cys^3 ($\chi_1 = -48 \pm 6$), Arg^{11} ($\chi_1 = -52 \pm 25$) and Cys^{12} ($\chi_1 = -67 \pm 46$) are also observed and can result from the different refinement procedures used. The models of α-ImI, R7A analog and peptide II present a great homogeneity of their backbone (N, Cα, C) atoms and adopt helicoidal motifs. This result confirms the Hα's upfield trend clearly illustrated when calculating the secondary Hα chemical shifts (data not shown). Models of R7A analog consists in a well-defined 3D structure composed of a 3_{10}-helix involving residues Cys^2 to Ser^4 followed by a regular α-helix (as detected by the MOLMOL program [27]) comprising residues Pro^6 to Ala^9. These secondary structures appear in 25 of the 28 models calculated and only three models present a lack of 3_{10}-helix in the first loop. As for α-ImI, the edifice of the R7A analog is stabilized by multiple hydrogen bonds, of either *i*, *i*+3 ($CO(Gly^1)$-$NH(Ser^4)$, $CO(Cys^2)$-$NH(Asp^5)$, $CO(Asp^5)$-$NH(Cys^8)$, $CO(Cys^8)$-$NH(Arg^{11})$ and $CO(Ala^9)$-$NH(Cys^{12})$) or *i*, *i*+4 ($CO(Asp^5)$-$NH(Ala^9)$, $CO(Pro^6)$-$NH(Trp^{10})$ and $CO(Cys^8)$-$NH(Cys^{12})$). The R7A analog displays exactly the same combination of ϕ, ψ and χ_1 dihedral angles to that of α-ImI (data not shown). These results agree with the CD measurements and confirm the crucial role of the Arg^7 side chain for the α-ImI affinity [9,10]. Furthermore, it can be noticed that the side chain of residue Arg^{11} lies parallel to the Trp^{10} aromatic ring, explaining the peculiar chemical shifts observed the Arg^{11} side chain. Models of peptide II describe the same scaffold as those of α-ImI with lower structural order as shown from its atomic rmsd in Table 1. While the mean structure is still composed of an α-helix comprising residues Pro^6 to Ala^9, this α-helix appears only in 14 of the 32 structures. Twelve other structures present an additional 3_{10}-helix comprising residues Cys^2 to Ser^4. Six other structures present either a longer α-helix from residue Pro^6 to Arg^{11}, or only a 3_{10}-helix in the first loop or no well-defined secondary structures at all. Models of peptide II are stabilized by the same hydrogen bonds described for α-ImI and R7A analog except for the absence of *i*, *i*+2 (including a Asp^5-Arg^7 salt bridge) and *i*, *i*+3 ($CO(Arg^7)$-HN(side chain of Trp^{10})) and $CO(Ala^9)$-$HN(Cys^{12})$ hydrogen bonds. These results correlate with the loss of helical contribution at 222 nm measured on CD spectra. Finally, peptide II differs from the wild type α-ImI and the R7A analog by the orientation of the tryptophan side chain. The tryptophan indole ring that faced Arg^{11} side chain in the native α-ImI and R7A analog is rejected to the opposite face of the molecule as shown in Fig. 3. This correlates with the changes of the chemical shifts observed for the Arg^{11} side chain protons. Clearly, the different orientation of the W^{10} indole ring in peptide II does not affect its binding affinity comparing to that of α-ImI [9]. This observation could be explained by the decrease of the conformational entropy of peptide II on binding to the receptor. The good fit of the $D^5P^6R^7$ active site of peptide II on the α7 n-AchR could counterbalance this decrease and enabled the reverse orientation of the W^{10} indole ring in peptide II. The compared NMR structures confirm the structural importance of the Cys^2,Cys^8 disulfide bridge that blocks the conformation of the $D^5P^6R^7$ sequence in the first loop of the α-ImI conotoxin. The second loop of α-ImI even opened by the Cys^3,Cys^{12} disulfide deletion did not affect the affinity of the toxin, e.g. peptide II.

A question arises on the selective targets of the two α-conotoxins, α-ImI [2] and α-EpI [3]. The two toxins share the same N-terminal sequence $G^1CCSDPRC^8$ in the first loop but display a different sequence and size for the second loop (Fig. 1). According to the recently resolved 3D structure of α-ImI [11,12] and in α-EpI [35], their first loop structures are identical. Therefore, the selectivity of these two conotoxins for various neuronal subtypes could be due to the nature of the side chains and the conformation of their second loop. The confirmation of this hypothesis will be supported by further binding studies of α-EpI mutants in its second loop. Moreover, given that α-EpI targets the α3β2, α3β4 n-AchR subtypes in bovine chromaffin cells [5], a comparative binding study of α-EpI and α-ImI on pure recombinant α7 n-AchR subtype will be relevant for their respective selectivity.

Acknowledgements: Co-ordinates have been deposited at the Protein Data Bank at Brookhaven National Laboratories. This work was supported by a post-doctoral grant to C.J.-M. from the Conseil Régional d'Auvergne (bourses Excellence), France which is gratefully acknowledged.

References

[1] Myers, R.A., Cruz, L.J., Rivier, J.E. and Olivera, B. (1993) Chem. Rev. 93, 1923–1936.
[2] McIntosh, J.M., Yoshikami, D., Mahe, E., Nielsen, D.B., Rivier, J.E., Gray, W.R. and Olivera, B.M. (1994) J. Biol. Chem. 269, 16733–16739.
[3] Loughnan, M., Bond, T., Atkins, A., Cuevas, J., Adams, D.J., Broxton, N.M., Livett, B.G., Down, J.G., Jones, A., Alewood, P.F. and Lewis, R. (1998) J. Biol. Chem. 273, 15667–15674.
[4] Cartier, G.E., Yoshikami, D., Gray, W.R., Luo, S., Olivera, B.M. and McIntosh, JM. (1996) J. Biol. Chem. 271, 7522–7528.
[5] Luo, S., Kulak, J.M., Cartier, G.E., Jacobsen, R.B., Yoshikami, D., Olivera, B.M. and McIntosh, J.M. (1998) J. Neurosci. 18, 8571–8579.
[6] Fainzilber, M., Hasson, A., Oren, R., Burlingame, A.L., Gordon, D., Spira, M.E. and Zlotkin, E. (1994) Biochemistry 33, 9523–9529.
[7] Johnson, D.S., Martinez, J., Elgoyhen, A.B., Heineman, S.F. and McIntosh, J.M. (1995) Mol. Pharmacol. 48, 194–199.
[8] Pereira, E.F.R., Alkondon, M., McIntosh, J.M. and Albuquerque, E.X. (1996) J. Pharmacol. Exp. Ther. 278, 1472–1483.
[9] Servent, D., Lamthanh, H., Antil, S., Bertrand, D., Corringer, P.J., Changeux, J.P. and Ménez, A. (1998) J. Physiol. (Paris) 92, 107–111.
[10] Quiram, P.A. and Sine, S.M. (1998) J. Biol. Chem. 273, 11001–11006.
[11] Maslennikov, I.V., Shenkarev, Z.O., Zhmak, M.N., Ivanov, V.T., Methfessel, C., Tsetlin, V.I. and Arseniev, A.S. (1999) FEBS Lett. 444, 275–280.
[12] Rogers, J.P., Luginbühl, P., Shen, G.S., McCabe, R.T., Stevens, R.C. and Wemmer, D.E. (1999) Biochemistry 38, 3874–3882.
[13] Lamthanh, H., Virelizier, H. and Frayssinhes, D. (1995) Peptide Res. 8, 316–320.
[14] Servent, D., Winckler-Dietrich, V., Hu, H.Y., Kessler, P., Drevet, P., Bertrand, D. and Ménez, A. (1997) J. Biol. Chem. 272, 24279–24286.
[15] Rance, M., Sørensen, O.W., Bodenhausen, G., Wagner, G., Ernst, R.R. and Wüthrich, K. (1983) Biochem. Biophys. Res. Commun. 117, 479–485.
[16] Braunschweiler, L. and Ernst, R.R. (1983) J. Magn. Reson. 53, 521–528.
[17] Davis, D.G. and Bax, A. (1985) J. Am. Chem. Soc. 107, 2820–2821.
[18] Jeener, J., Meier, B.H., Bachman, P. and Ernst, R.R. (1979) J. Chem. Phys. 71, 4546–4553.

[19] Macura, S., Hyang, Y., Suter, D. and Ernst, R.R. (1981) J. Magn. Reson. 43, 259–281.
[20] Pons, J.L., Malliavin, T.E. and Delsuc, M.-A. (1996) J. Biomol. NMR 8, 445–452.
[21] Griesinger, C., Otting, G., Wüthrich, K. and Ernst, R.R. (1988) J. Am. Chem. Soc. 110, 7870–7872.
[22] Piotto, M., Saudek, V. and Sklenar, V. (1992) J. Biomol. NMR 2, 661–666.
[23] Sklenar, V., Piotto, M., Leppik, R. and Saudek, V. (1993) J. Magn. Reson. A 102, 241–245.
[24] Marion, D., Ikura, M., Tschudin, R. and Bax, A. (1989) J. Magn. Reson. 85, 393–399.
[25] Krimm, I., Gilles, N., Sautiere, P., Stankiewicz, M., Gordon, D. and Lancelin, J.-M. (1999) J. Mol. Biol. 285, 1749–1763.
[26] Brünger, A.T. (1996) X-PLOR Version 3.851. Yale University Press, New Haven, CT.
[27] Koradi, R., Billeter, M. and Wüthrich, K. (1996) J. Mol. Graphics 14, 51–55.
[28] Brahms, S. and Brahms, J. (1980) J. Mol. Biol. 138, 149–178.
[29] Woody, R.W. (1974) in: Peptides, Polypeptides and Proteins (Blout, E.R., Bovey, F.A., Lotan, N. and Goodman, M., Eds.), pp. 338–350, Wiley, New York.
[30] Perczel, A., Hollosi, M., Sandor, P. and Fasman, G.D. (1993) Int. J. Peptide Protein Res. 41, 223–236.
[31] Hutchinson, E.G. and Thornton, J.M. (1994) Protein Sci. 3, 2207–2216.
[32] Woody, R.W. (1978) Biopolymers 17, 1451–1467.
[33] Hollosi, M., Köver, K.E., Holly, S., Radics, L. and Fasmann, G.D. (1987) Biopolymers 26, 1555–1572.
[34] Wütrich, K. (1986) NMR of Proteins and Nucleic Acids, Wiley Interscience, New York.
[35] Hu, S.H., Loughnan, M., Miller, R., Weeks, C.M., Blessing, R.B., Alewood, P.F., Lewis, R.J. and Martin,,J.L. (1998) Biochemistry 37, 11425–11433.